JOURNAL OF NATURAL PRODUCTS

Article

pubs.acs.org/jnp

Ribifolin, an Orbitide from *Jatropha ribifolia*, and Its Potential Antimalarial Activity

Meri Emili F. Pinto,*[,†] João M. Batista, Jr.,[†,‡] Johannes Koehbach,[§,⊥] Pratibha Gaur,[∥] Abhinay Sharma,[∥] Myna Nakabashi,[∥] Eduardo Maffud Cilli,[†] Guilherme M. Giesel,[#] Hugo Verli,[#] Christian W. Gruber,[⊥] Ewan W. Blanch,[‡] Joseam F. Tavares,[□] Marcelo S. da Silva,[□] Celia R. S. Garcia,[∥] and Vanderlan S. Bolzani*[,†]

[†]Institute of Chemistry, São Paulo State University-UNESP, 14800-060, Araraquara, São Paulo, Brazil

[‡]Manchester Institute of Biotechnology and Faculty of Life Sciences, The University of Manchester, M1 7DN, Manchester, United Kingdom

[§]School of Biomedical Sciences, The University of Queensland, 4072, St. Lucia, Queensland, Australia

[⊥]Center for Physiology and Pharmacology, Medical University of Vienna, 1090, Vienna, Austria

[∥]Departament of Physiology, Institute of Biosciences, The University of São Paulo-USP, 05508-900, São Paulo, Brazil

[#]Center of Biotechnology, Federal University of Rio Grande do Sul-UFRGS, 91500-970, Porto Alegre, Rio Grande do Sul, Brazil

[□]Laboratory of Pharmaceutical Technology, Federal University of Paraíba-UFPB, 58051-970, João Pessoa, Paraíba, Brazil

Supporting Information

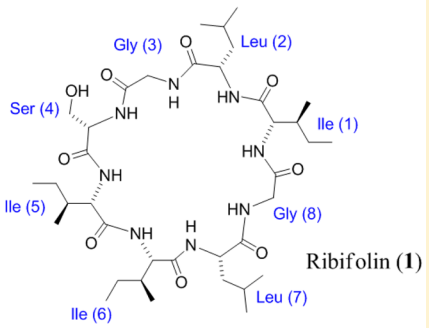

ABSTRACT: A new orbitide named ribifolin was isolated and characterized from *Jatropha ribifolia* using mass spectrometry, NMR spectroscopy, quantitative amino acid analysis, molecular dynamics/simulated annealing, and Raman optical activity measurements and calculations. Ribifolin (**1**) and its linear form (**1a**) were synthesized by solid-phase peptide synthesis, followed by evaluation of its antiplasmodial and cytotoxicity activities. Compound **1** was moderately effective (IC_{50} = 42 μM) against the *Plasmodium falciparum* strain 3D7.

Jatropha ribifolia (Pohl) Baill. (syn. *Adenoropium ribifolium* Pohl, *Jatropha gossypifolia* var. *ribifolia* (Pohl) Müll.), commonly known as "pinhão-manso" and "pinhão rasteiro", belongs to the Euphorbiaceae family, subfamily Crotonideae.[1] According to ethnopharmacological studies, its latex is widely used throughout northeastern Brazil as a traditional herbal medicine due to its antivenom activity.[2] Additionally, its seeds are sold in markets in the region for oil production and are also used as a purgative for veterinary use.[2,3] The genus *Jatropha* is a rich source of Caryophyllaceae-type cyclopeptides,[4] recently redefined as orbitides.[5] The term "orbitide" was introduced for all N-to-C cyclized peptides from plants that do not contain disulfides linkages.[5] These compounds exhibit a wide range of biological activities[6,7] possibly due to their target specificity, high affinity, and metabolic stability,[8] as well as by mimicking protein structural patterns. Thus, orbitides may be considered as a naturally occurring library of "privileged structures".

The CyBase database (www.cybase.org.au), dedicated to providing Web tools and information about cyclic peptides to the scientific community,[9] currently contains 108 Caryophyllaceae-type cyclopeptide sequence entries, of which 11 are from the genus *Jatropha*; additionally, another eight sequences were described in the literature.[7] Orbitides (Caryophyllaceae-type) have been shown to have cytotoxic, antiplatelet, antimalarial, immunomodulating, antiproliferative,[5] and protease-inhibiting

Special Issue: Special Issue in Honor of William Fenical

Received: October 6, 2014
Published: February 20, 2015

DOI: 10.1021/np5007668
J. Nat. Prod. 2015, 78, 374−380

Table 1. ^{1}H (500 MHz) and ^{13}C NMR (125 MHz) Data for Ribifolin (1) in DMSO-d_6[a]

	position		δ_C, mult.	δ_H, mult. (J in Hz)	COSY	NOESY	HMBC
Ile_1	1	NH		7.34	3	3, 4, 6, 25, 46, 51, 52	
	2	CO	172.29, C				
	3	α	55.95, CH	4.40, t (8.0)	4	1, 4, 6, 7, 8, 10, 13	2, 4, 6, 7, 50
	4	β	36.61, CH	1.84, m		1, 3, 6, 7, 8, 23, 24, 25	3, 7
	5	γ	15.15, CH_3	0.75[b]			
	6	γ'	23.45, CH_2	1.22, m		1, 3, 4, 5	5, 7
	7	δ	10.77, CH_3	0.72[b]			4, 6
Leu_2	8	NH		8.65[b]		1, 3, 4, 6, 11, 25	2, 10, 11
	9	CO	172.20, C				
	10	α	53.22, CH	3.76[b]	11	8, 12, 14	9, 11
	11	βa	38.90, CH_2	1.55[b]		8, 10, 14	9,10, 11, 15
	12	βb		1.42[b]		8, 10	15
	13	γ	40.06, CH	1.50[b]			
	14	δ	21.76, CH_3	0.84[b]			
	15	δ'	22.86, CH_3	0.88[b]			
Gly_3	16	NH		8.64[b]	18, 19	10, 19, 20, 22	9, 18
	17	CO	168.71, C				
	18	αa	42.71, CH_2	3.88, d (7.5)		19	9, 17
	19	αb		3.36[b]		18	
Ser_4	20	NH		7.62, d, (9)	22	4, 6, 19, 22, 23, 24, 25	9, 17
	21	CO	170.92, C				
	22	α	53.05, CH	4.78, m	23	20, 23, 24, 25, 26, 32, 33	17, 21, 23
	23	βa	62.91, CH_2	3.57, m			21, 22
	24	βb		3.76, m		20, 22, 25	21
	25	OH		5.84, br s			
Ile_5	26	NH		8.25[b]		22, 34	
	27	CO	170.73, C				
	28	α	58,75, CH	4.04, m	29	22, 26, 29, 31, 33, 34	27, 29, 31
	29	β	35.18, CH	1.95, m		26, 28, 32, 33	
	30	γ	15.78, CH_3	0.87[b]			
	31	γ'a	24.35, CH_2	1.25[b]		26, 29, 33	33
	32	γ'b		1.36[b]		26, 29, 33	33
	33	δ	11.93, CH_3	0.84[b]			
Ile_6	34	NH		7.75[b]		23, 25, 36, 37, 39, 40	
	35	CO	171.72, C				
	36	α	57.51, CH	3.92[b]	37	26, 34, 37, 39, 40	35, 37, 38, 39
	37	β	34.94, CH	1.69[b]		25, 32, 34, 36, 39, 40	35, 36, 38, 39
	38	γ	15.03, CH_3	0.78[b]			
	39	γ'	25.04, CH_2	1.10, m		34, 36, 38	36, 37, 38, 40
	40	δ	10.14, CH_3	0.77[b]			
Leu_7	41	NH		7.73[b]		36, 43	
	42	CO	172.56, C				
	43	α	52.40, CH	3.99, m	46	1, 41, 44, 47, 49	42, 44
	44	βa	40.06, CH_2	1.42[b]			
	45	βb		1.54[b]		41	
	46	γ	40.00, CH	1.50[b]		41, 43	
	47	δ	21.52, CH_3	0.81[b]			
	48	δ'	22.79, CH_3	0.87[b]			
Gly_8	49	NH		8.26[b]		1, 43, 46, 52	
	50	CO	168.82, C				
	51	αa	42.80, CH_2	3.91[b]	52	1, 41, 44, 52	50
	52	αb		3.32, d (4.5)		51	50

[a]Assignments of the ^{13}C and ^{1}H signals were made on the basis of DEPT, COSY, TOCSY, HSQC, HMBC, and NOESYspectroscopic data; data reported in ppm. [b]Overlapped by other signals.

activities.[10] They were also found to interact with molecular membranes.[11] Certain natural orbitides, such as curcacycline B (IC_{50} = 10 mM), pohlianins A (57 μM), B (25 μM), and C (16 μM), mahafacyclins A (16 μM) and B (2.2 μM), and chevalierin A (8.6 μM), are active against *Plasmodium falciparum* (see Tables 1 and 2), a protozoan that causes the most severe form of the malaria disease.[7] Furthermore, *P. falciparum* and *P. vivax* are presently subject to a renewed global research initiative, aiming to identify targets for prophylaxis and treatment of malaria caused by these

DOI: 10.1021/np5007668
J. Nat. Prod. 2015, 78, 374−380

Table 2. Orbitides Isolated from *Jatropha* Species and their Potential Antiplasmodial Activity

species	compounds	sequences	antiplasmodial activity (IC_{50}, μm])	references
Jatropha ribifolia	ribifolin (**1**)	cyclo ILGSIILG	42	this study
Jatropha curcas	curcacycline B	cyclo ILGSPILLG	10 000	23, 24
Jatropha chevalieri	chevalierin A	cyclo IMGIPILA	9	25
Jatropha mahafalensis	mahafacyclin A	cyclo VFGTILG	16	26
Jatropha mahafalensis	mahafacyclin B	cyclo FFGTFFG	2	22
Jatropha pohliana	pohlianin A	cyclo VLLYPLG	57	6
Jatropha pohliana	pohlianin B	cyclo LLLYPLG	25	6
Jatropha pohliana	pohlianin C	cyclo FGGTIIFG	16	6

parasites.[12] The mortality rate of the disease is very high, and today the parasites have gained resistance to available drugs, which has increased the urgency for finding new treatments to fight malaria.[13]

Research dealing with antimalarial activity of orbitides is still sparse despite previous good results.[7] Therefore, the main goals of this work were to isolate and structurally characterize compound **1** as well as to examine its antiplasmodial activity against *P. falciparium* and cytotoxic properties on human HEK293T cells.

RESULTS AND DISCUSSION

Following the solvent extraction of the aerial parts of *Jatropha ribifolia* and repeated purification steps, compound **1** was isolated as an amorphous white solid (2 mg, 1% wet weight) that tested positive for the chlorine-*o*-tolidine reagent, which is used for detection of peptide amide groups.[14] This reagent is carcinogenic to humans and, therefore, care should be exercised in its use in the laboratory.[15] Additionally, the negative reaction with ninhydrin showed the absence of a free amino group, thus indicating a cyclic peptide structure.[16] The molecular formula was established as $C_{37}H_{66}N_8O_9$, based on HRESIMS (observed $[M + H]^+$ m/z 767.4756; calcd m/z 767.4764), 1D and 2D ^1H and ^{13}C NMR spectroscopic data as well as amino acid analysis.

From MS/MS analysis, the loss of a water molecule was observed (i.e., open ring) m/z 749.5054, followed by subsequent losses of amino acid residues: m/z 636.4104 (Ile/Leu), m/z 523.3267, (Ile/Leu), m/z 466.3043 (Gly), m/z 353.2248 (Ile/Leu), m/z 239.1794 (Ile/Leu), respectively (see Figure S4, Supporting Information). Amino acid analysis of the hydrolysates of **1** showed the molar ratio of the four different amino acids: Ser, Gly, Leu and Ile. The ^1H NMR spectrum (measured in DMSO-d_6) showed eight downfield amide proton signals at δ 8.65−7.35, one proton of a Ser-hydroxyl group at δ 5.84 and α-protons between δ 3.3 and 4.8. The ^{13}C NMR spectrum showed seven carbonyl signals (δ 168.7 to 172.5) and eight carbon resonances in the region δ 42.6−58.7. The ^{13}C and ^1H chemical shift assignments for the amino acid residues of **1** in DMSO-d_6 are listed in Table 1.

Detailed analysis of the TOCSY spectra showed complete scalar spin−spin coupling patterns for all the amino acids (Figures S7−S10). The NOESY spectrum allowed sequential assignments of adjacent amino acid residues [dNN(i,i+1) and dαN(i,i+l)]. Inter-residue dαN(i,i+l) connectivities were found between Ile1-NH and Leu_2-NH, Leu_2-NH and Ile_1-Hα, Gly_3-NH and Leu_2-Hα, Gly_3-NH and Ser_4-NH, Ser_4-NH and Gly_3-Hα, Ile_5-NH and Ser_4-Hα, as well as Ile_5-NH and Ile_6-NH (Figure S16). Additionally, for sequencing purposes, the HMBC analysis showed key correlations between Ile_1-NH and Gly_8-CO, Ile_1-NH and Gly_8-CO, Leu_2-NH and Ile_1-CO, Gly_3-NH and Leu_2-CO, Ser_4-NH and Gly_3-CO, Ile_5-NH and Ser_4-CO, Ile_6-NH and Ile_5-CO, as well as Gly_8-NH and Ile_7-CO (Figure S19) (Table 1).

The combination of HRESIMS data, amino acid analysis, TOCSY, COSY, NOESY, HSQC, and HMBC spectra interpretation allowed us to identify the eight residues of **1** (see Supporting Information), outlining its sequence as cyclo-ILGSIILG (Figure 1).

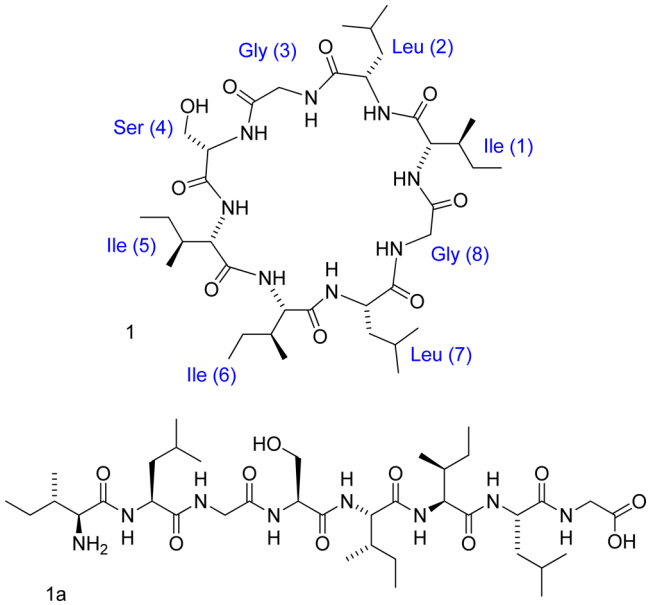

Figure 1. Structure of ribifolin (**1**) and the amino acid sequence of linear ribifolin (**1a**).

Simulated annealing molecular dynamics (SA/MD) allows the generation of multiconformer models that can represent molecular motion and discrete disorder toward molecule conformation. In this sense, the structural dynamics of natural **1** with all interproton distances according to NOESY spectroscopic data were retrieved from major cluster conformation after SA/MD processing and show the structure of the cyclic peptide with its backbone assuming a twisted ring shape (Figure S1, see Supporting Information for more details).

After isolation, sequencing, structural elucidation, and SA/MD conformational analysis of **1**, the synthesis of this peptide was performed to confirm the proposed sequence and to obtain additional material for biological tests as well as Raman optical activity (ROA) measurements.

Furthermore, a linear ribifolin analogue (**1a**) was synthesized as an intermediate and used for determining the role of the circular backbone for its bioactivity. The synthesis of **1** was accomplished using a solid-phase technique (SPPS), based on the 9-fluorenylmethyloxycarbonyl (Fmoc) strategy[17] using

DOI: 10.1021/np5007668
J. Nat. Prod. 2015, 78, 374−380

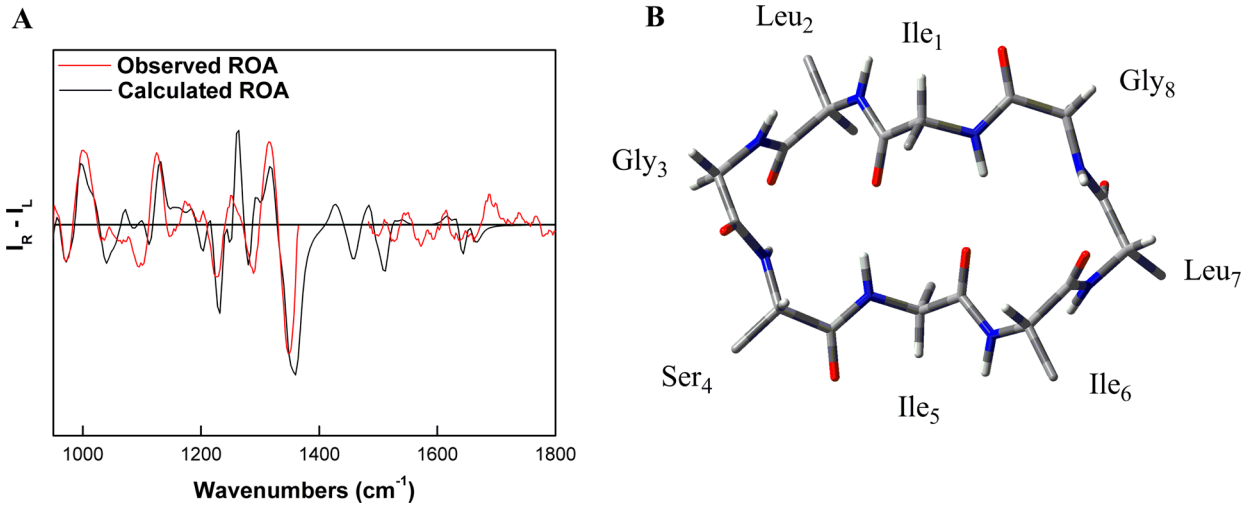

Figure 2. (A) Observed and calculated ROA spectra of synthetic ribifolin (**1**) at the B3LYP/6-311+G(d)//B3LYP/6-311+G(d) level in water using PCM. Deleted spectral region corresponds to overlapping signals from acetonitrile CH_3 deformation modes. (B) Backbone structure of the lowest energy conformer identified for **1** lacking side-chain atoms.

glycine at the C-terminal position to prevent racemization during cyclization. After the complete chain assembly, the linear peptide was cleaved from the solid support by using diluted trifluoroacetic acid (TFA) and precipitation in diethyl ether. The material was lyophilized, diluted in 1 mM DMF, and then cyclized by means of HBTU/HOBT/DIEA (1.5; 1.5; 4.5 equiv × 2 h). In this reaction, the amino group of Ile_1 acts as a nucleophile to displace the hydroxyl group of Gly_8 forming a peptide bond (head-to-tail cyclization). The reaction was completed under high dilution conditions (1 mM, peptide in DMF) in order to minimize unwanted intermolecular reactions such as oligo- and polymerizations and to improve the soluble yield of the cyclic peptide. The success of this total synthesis was confirmed by NMR spectroscopic analysis (Figure S25). Overall, this synthetic methodology provided yields of 83% and 51% for linear **1a** and cyclic **1**, respectively. The native and synthetic cyclic peptides showed identical molecular weight, HPLC retention times (Figure S3), and NMR spectroscopic data (Figures S23−S26) as well as very similar values of optical rotation ($[\alpha]^{23}_D$ = −20 for natural and $[\alpha]^{23}_D$ = −19 for synthetic orbitide **1**, *c* 0.06, CH_3CN). The abundant yield of the synthetic peptide, compared with that obtained by extraction (i.e., 20 mg·kg^{-1} dry plant) of natural **1**, encourages the use of SPPS in order to obtain peptides in reasonable quantities for use in complementary studies.

In order to complement the SA/MD conformational analysis, measurements and calculations of Raman optical activity were carried out. ROA, which measures a small difference in the intensity of vibrational Raman scattering from chiral molecules in right- and left-circularly polarized incident light, scattered light, or both,[18] is a very informative chiroptical tool for solution-state conformational analysis of peptides and proteins in different solvents.[19] With the aid of state-of-the-art calculations of ROA spectra using density functional theory (DFT) methods, it is also possible to determine the absolute configuration of chiral molecules.[20] The very good agreement between experimental and calculated data in the amide III region (Figure 2) confirmed the all-L absolute configuration of the synthetic cyclic peptide, which was then used to assign the stereochemistry of natural **1** based on their nearly identical optical rotation values. Additionally, one main lowest energy conformer was identified, contributing 90% of the total Boltzmann distribution. Good correspondence of the calculated ROA spectrum for this conformer, with respect to experimental data, also indicated that, in partially aqueous solution, **1** adopts a backbone structure with two γ-turns, one being classical (between Leu_2-CO and Ser_4-NH) and one inverse (between Ile_6-CO and Gly_8-NH), connecting two hydrogen-bonded residues (Ile_1 and Ile_5) with a set of phi/psi angles typical of β-strand-forming residues (Figure 2).

After detailed structural analysis, the synthetic linear (**1a**) and cyclic (**1**) peptides were evaluated for their antiplasmodial activity, with chloroquine being used as the positive control (IC_{50} = 0.3 μM) for these dose−response experiments. Compound **1** (IC_{50} = 42 μM) was moderately effective against the *P. falciparum* 3D7 strain, whereas linear **1a** (IC_{50} = 519 μM) showed a weak effect in inhibiting the survival of the parasites. Since the cyclization of peptides is responsible for minimization of conformational freedom of the peptide structure, it often results in a higher target affinity by reducing unfavorable entropic effects, thus enhancing their biological activity.[21] Interestingly, the antiplasmodial activity obtained for compound **1** was significantly higher than that reported for another orbitide, the nonapeptide curcacycline B (IC_{50} = 10 mM).[22] Curcacycline B has an amino acid sequence very similar to that of **1**, differing only in two positions, i.e., an additional proline at position 4 and a leucine instead of an isoleucine at position 6 (Table 2). Apparently, the additional *trans*-configured[23] proline residue of curcacycline B is detrimental to its antiplasmodial activity. This effect seems to be even more important than the opening of the orbitide backbone ring given the fact that **1a** is more active than curcacycline B. It is noteworthy to mention, however, that these peptides have not been evaluated in the same assay. A comparison of amino acid sequence and antiplasmodial activity of orbitides from various *Jatropha* species including curcacycline B is shown in Table 2.

Additionally, synthetic **1a** and **1** were assessed for their unspecific cytotoxicity toward human embryonic kidney cells (HEK293T). This was done by monitoring the number of living cells at the same concentrations used to evaluate antiplasmodial activity. No cytotoxicity, but normal growth,

DOI: 10.1021/np5007668
J. Nat. Prod. 2015, 78, 374−380

was observed in the tested concentration range (0.001−100 μM).

Thus, in this study, we reported the isolation and structural elucidation of the new octapeptide ribifolin (**1**) from *J. ribifolia*. NMR spectroscopic analysis as well as molecular dynamics simulations indicated its backbone structure as having a twisted-ring shape. Additionally, analyses of experimental and calculated ROA spectra provided further insights into the configuration and solution secondary structure of **1**. The synthesis of the natural cyclic peptide **1** and its linear analogue **1a** was accomplished by SPPS strategy, and their growth inhibitory activities against the *P. falciparum* 3D7 strain were tested. Compound **1** was moderately effective against the parasite, with an IC_{50} of 42 μM, whereas its linear analogue **1a** had an IC_{50} of 519 μM, which provided evidence for the importance of cyclization to improve biological activity. The cytotoxic activity was also measured, but none of the tested compounds exhibited any cytotoxicity against human cells. This result is very stimulating for further studies on orbitides from Brazilian Euphorbiaceae.

EXPERIMENTAL SECTION

General Experimental Procedures. Optical rotations were recorded in acetonitrile solutions on a Schimidt-Haensch (Berlin, Germany) Polartronic H-100 polarimeter using quartz cells of 1 dm path length at 23 °C. ^{1}H (500 MHz), ^{13}C (125 MHz), DEPT, COSY, HSQC, HMBC, TOCSY, and NOESY NMR spectra were acquired at room temperature on a Varian (Palo Alto, CA, USA) Inova 500 spectrometer instrument with DMSO-d_6 as the solvent. Spectra were referenced to residual solvent signals with resonances at δH 2.49 and δC 39.7 and tetramethylsilane as internal standard. High-resolution ESIMS spectra were obtained with a Bruker Daltonics (Billerica, MA, USA) UltrOTOF-Q spectrometer using (N_2) 10 eV for MS and 45 eV for MS/MS in positive ionization mode. Analytical HPLC analysis was carried out on a Shimadzu (Tokyo, Japan) Prominence SPD M20A instrument with a KROMASIL (Bohus, Sweden) C_{18} column (4.6 × 250 mm, 100 Å pore size, 5 μm particle size, 1 mL·min^{-1}). Semipreparative purifications were carried out on a C_{18} Phenomenex (Torrance, CA, USA) AXIA Packed LUNA column (250 × 21.20 mm, 100 Å pore size, 5 μm particle size, 8 mL·min^{-1}). Amino acid analyses were carried out on a Shimadzu (Kyoto, Japan) LC-10A/C-47A automated analyzer. HPLC eluates were monitored using UV-detection at wavelengths of 220 and 280 nm. Absorbance for the cytotoxic assay was determined at 570 nm using a Molecular Devices (Sunnyvale, CA, USA) Flexstation multiplate reader. ROA spectra were recorded using a BioTools (Jupiter, FL, USA) Chiral Raman spectrometer operated via Critical Link (Syracuse, NY, USA) LLC software. The instrument was set up with a scattered circular polarization strategy in backscattering geometry using a Millennium (Neath, UK) Pro Nd−VO_4 laser with an excitation wavelength of 532 nm, laser power of 600 mW at the sample, spectral resolution of 7 cm^{-1}, sample concentration of 40 mg·mL^{-1} in 50:50 H_2O−CH_3CN, and spectral acquisition time of 35 h.

Plant Material. Aerial parts of *Jatropha ribifolia* (Pohl) Baill. (Euphorbiaceae) were collected in September 2009 in the semiarid northeastern region of Brazil at Pico do Jabre localized in the city of Maturéia in Paraiba State, 7°15′30″ S, 37°23′30″ W. A voucher specimen (Agra, no. 7243) is stored at the Herbarium of Prof. Lauro Pires Xavier, Federal University of Paraíba, João Pessoa-PB, Brazil.

Extraction and Isolation. Dry and pulverized plant material (100 g) was extracted exhaustively with EtOH−H_2O (95:5, v/v) at room temperature. The solvent was then removed under reduced pressure, resulting in 2 g of crude extract, which was subsequently extracted with EtOAc, resulting in a 200 mg fraction. The fraction was dissolved in H_2O−CH_3CN (1 mL, 3:1, v/v) and further fractionated on a Strata C_{18}−E solid-phase extraction cartridge (Phenomenex) using H_2O and CH_3CN as mobile phases, with a decreasing polarity gradient (0%, 30%, 70%, and 100% CH_3CN in H_2O). Each resulting fraction was analyzed using analytical HPLC employing a linear gradient from 5−95% of solvent B (CH_3CN containing 0.036% TFA) in solvent A (H_2O containing 0.045% TFA) for 60 min with simultaneous detection using Cl_2−3,3′-dimethylbenzidine (*o*-tolidine reagent); the fraction of 70% CH_3CN was selected. Further purification of this fraction was carried out by semipreparative HPLC using a linear gradient of 40−80% of solvent B in solvent A in 120 min; fractions of 10 mL were collected. The aqueous solution of fraction 1B was subsequently lyophilized to yield ribifolin (**1**) (2.0 mg).

*Ribifolin (**1**):* white, amorphous solid; $[\alpha]^{23}_D$ −20 (*c* 0.06, ACN); ^{1}H and ^{13}C NMR data (see Table 1); HRESIMS $[M + H]^+$ *m/z* 767.4756 (calcd for $C_{37}H_{67}N_8O_9$, *m/z* 767.4764), $[M + Na]^+$ *m/z* 789.4576, $[M + K]^+$ *m/z* 805.4296, and $[M - OH]^+$ *m/z* 749.5054.

Amino Acid Composition. Purified ribifolin (**1**) (0.5 mg) was hydrolyzed in 6 M HCl (1 mL) in a sealed tube at 110 °C for 72 h. After hydrolysis, HCl was removed under reduced pressure, and the residual material was dissolved in a 0.2 M Na^+-citrate buffer (pH 2.2). The amino acid content was determined by cation-exchange chromatography using an automated amino acid analyzer with *ortho*-phthalaldehyde as detection reagent.

Solid-Phase Peptide Synthesis of Ribifolin. The linear precursor of ribifolin (**1a**) was synthesized manually according to a standard Nα-Fmoc protecting-group strategy using solid-phase peptide synthesis (SPPS). Synthesis was performed starting with the Fmoc-L-Gly Wang resin (Novabiochem, 0.55 mmol·g^{-1}) on the scale of 0.4 mmol. The α-amino group deprotection steps were performed in 20% piperidine−DMF for 20 min. The L-amino acids were coupled in excess (0.8 mmol) using diisopropylcarbodiimide−*N*-hydroxybenzotriazole in 50% DCM−DMF (v/v). After a 2 h coupling time, the ninhydrin test was performed to estimate the completeness of the reaction. Cleavage from the resin and removal of side-chain protecting groups were simultaneously performed with TFA−*p*-cresol−H_2O (90:5:5) for 2 h. In this procedure, crude peptides were precipitated with anhydrous Et_2O, separated from soluble nonpeptide material by centrifugation, then extracted into 0.045% TFA in H_2O, and subsequently lyophilized (283 mg). Part of the crude linear peptide (**1a**) (150 mg) was next cyclized at a concentration of 1 mM in DMF, using 1.5 equiv of HBTU (*N*,*N*,*N*′,*N*′-tetramethyl-*O*-(1*H*-benzotriazol-1-yl)uronium hexafluorophosphate) and 10 equiv of DIEA (*N*,*N*-diisopropylethylamine). The reaction mixture was stirred for 2 h at RT. The solution was diluted with H_2O and partitioned 5-fold with EtOAc. The organic phases were combined, washed with H_2O (5×), then concentrated, and lyophilized (106 mg). The crude cyclic peptide (**1**) was dissolved in 0.045% TFA in H_2O−0.036% TFA in CH_3CN (7:3, v/v) and subsequently purified by reversed-phase semi-preparative HPLC. The homogeneity of the peptides was analyzed by reversed-phase analytical HPLC. The molecular weight and amino acid composition of synthetic ribifolin (**1**) was confirmed by ESIMS and amino acid analysis.

Raman Optical Activity Calculations. All DFT and time-dependent DFT calculations were carried out at 298 K in water solution using the polarizable continuum model (PCM) incorporated in Gaussian 09 software.[27] The all-L configuration of ribifolin (**1**) was arbitrarily chosen for the calculations. Conformational analysis was carried out at the molecular mechanics level of theory with the Monte Carlo algorithm using the MMFF force field implemented in Spartan 08 (Wavefunction, Irvine, CA, USA) software package. Fifty-one conformers with relative energy within 10 kcal·mol^{-1} of the lowest energy conformer were selected and further geometry optimized at the B3LYP/PCM/6-31G(d) level in water. The four conformers identified within an energy window of 2.1 kcal·mol^{-1}, corresponding to 90% of the total Boltzmann distribution, were selected for Raman (not shown) and ROA spectral calculations. ROA calculations were carried out using the so-called "one-step" approach[20] at the B3LYP/PCM/6-311+G(d) level in water. The incident light frequency was 532 nm. The Boltzmann factor for each conformer was calculated based on Gibbs free energy. Each spectrum was plotted as a sum of Lorentzian bands with half-widths of 10 cm^{-1}. The calculated wavenumbers were multiplied with a scaling factor of 0.98, and the Boltzmann-population-

DOI: 10.1021/np5007668
J. Nat. Prod. 2015, 78, 374−380

weighted composite spectra were plotted using Origin (OriginLab, Northampton, MA, USA) software.

In Vitro Cell Culture of *P. falciparum* (3D7). The well-known chloroquine-sensitive *P. falciparum* strain 3D7 was used in the present study. Chloroquine was used as a control for all experiments. Linear (**1a**) and cyclic (**1**) peptides were used for the study. Parasites were cultured and synchronized, maintained at 1−10% parasitaemia and 2% hematocrit in RPMI 1640 culture medium supplemented with erythrocytes, 10% human serum, 0.16% glucose, 0.2 mM hypoxanthine, 2.1 mM L-glutamine, and 22 mg·mL^{-1} gentamycin. Cultures were incubated at 37 °C, 3% O_2, 3% CO_2, and 94% N_2. Synchronization of parasites in culture to ring stages was carried out by repetitive treatment with 5% (w/v) sorbitol. Parasite growth and parasitaemia were monitored by assessing Giemsa-stained blood smears under the microscope.

Treatment (Antiplasmodial Activity Assay). The treatment experiments were conducted in 96-well plates with different concentrations (100, 20, 4, 0.8, 0.16, 0.032, 0.0064, and 0.00128 μM) for each compound in triplicate for each concentration. For this assay, 1% parasitaemia and 2% hematocrit were set in each well, and 200 μL of RPMI with 10% human serum and the compounds were added. The parasites were exposed to the compound and were incubated for 48 h. The concentration causing 50% inhibition (IC_{50}) was determined from the dose−response curves.

Cytotoxicity Assay. The toxicity of cyclic ribifolin (**1**) and synthetic linear peptide (**1a**) were evaluated in human embryonic kidney cells (HEK293T) using the MTT cell proliferation assay.[28] HEK cells (1×10^4/well) were seeded into 96-well plates and incubated in complete medium (DMEM supplemented with fetal calf serum) containing the antibiotics penicillin and streptomycin. After 24 h, the medium was replaced with fresh medium (100 μL/well), and the compounds were added in decreasing concentrations (100, 10, 1, 0.1, 0.01, and 0.001 μM). Cells were incubated with peptides for 48 h, and 20 μL of MTT reagent (5 mg·mL^{-1} of PBS) was added during the last 3 h of incubation. The absorbance at 570 nm was evaluated in a microplate reader.

Statistical Analysis. Prism (GraphPad, La Jolla, CA, USA) software was used for statistical analysis and to calculate IC_{50} values. All the experiments were conducted in triplicate and repeated three times independently to attain the final IC_{50} values.

■ ASSOCIATED CONTENT

Ⓢ Supporting Information

SA/MD simulations of **1**. HPLC profile, ^{1}H, ^{13}C, TOCSY, NOESY, HSQC, HMBC NMR spectra, and MS/MS of **1**. This material is available free of charge via the Internet at http://pubs.acs.org.

■ AUTHOR INFORMATION

Corresponding Authors

*(M. E. F. Pinto) E-mail: meriemily@hotmail.com.

*(V. S. Bolzani) Tel: 0055-16-33019660. Fax: 0055-16-33222308. E-mail: bolzani@iq.unesp.br.

Notes

The authors declare no competing financial interest.

■ ACKNOWLEDGMENTS

This work was supported by SISBIOTA-CNPq-FAPESP grant 2010/52327-5, CEPID-FAPESP grant 2013/07600-3, and CAPES grant BEX: 9875/11-5. The authors are also grateful to CNPq, CAPES, and FAPESP (2011/22339-4 and 2012/13739-1) for scholarships and financial support, as well as to Prof. M. de Fátima Agra (UFPB) for the identification of *J. ribifolia* plant material and to Prof. N. P. Lopes (USP-Ribeirão Preto) for HRESIMS measurements. This research was also supported by resources supplied by the Center for Scientific Computing (NCC/GridUNESP) of the São Paulo State University (UNESP).

■ DEDICATION

Dedicated to Dr. William Fenical of Scripps Institution of Oceanography, University of California−San Diego, for his pioneering work on bioactive natural products.

■ REFERENCES

(1) Leal, C. K. A.; Agra, M. F. *Acta Farm. Bonaerense* **2005**, *24*, 5−13.
(2) Agra, M. F.; Locatelli, E.; Rocha, E. A.; Baracho, G. S.; Formiga, S. C. *Rev. Bras. Farm.* **1996**, *77*, 97−102.
(3) Devappa, R. K.; Makkar, H. P. S.; Becker, K. *J. Am. Oil Chem. Soc.* **2011**, *88*, 301−322.
(4) Tan, N.-H.; Zhou, J. *Chem. Rev.* **2006**, *106*, 840−895.
(5) Arnison, P. G.; Bibb, M. J.; Bierbaum, G.; Bowers, A. A.; Bugni, T. S.; Bulaj, G.; Camarero, J. A.; Campopiano, D. J.; Challis, G. L.; Clardy, J.; Cotter, P. D.; Craik, D. J.; Dawson, M.; Dittmann, E.; Donadio, S.; Dorrestein, P. C.; Entian, K.-D.; Fischbach, M. A.; Garavelli, J. S.; Göransson, U.; Gruber, C. W.; Haft, D. H.; Hemscheidt, T. K.; Hertweck, C.; Hill, C.; Horswill, A. R.; Jaspars, M.; Kelly, W. L.; Klinman, J. P.; Kuipers, O. P.; Link, A. J.; Liu, W.; Marahiel, M. A.; Mitchell, D. A.; Moll, G. N.; Moore, B. S.; Müller, R.; Nair, S. K.; Nes, I. F.; Norris, G. E.; Olivera, B. M.; Onaka, H.; Patchett, M. L.; Piel, J.; Reaney, M. J. T.; Rebuffat, S.; Ross, R. P.; Sahl, H.-G.; Schmidt, E. W.; Selsted, M. E.; Severinov, K.; Shen, B.; Sivonen, K.; Smith, L.; Stein, T.; Süssmuth, R. D.; Tagg, J. R.; Tang, G.-L.; Truman, A. W.; Vederas, J. C.; Walsh, C. T.; Walton, J. D.; Wenzel, S. C.; Willey, J. M.; van der Donk, W. A. *Nat. Prod. Rep.* **2013**, *30*, 108−160.
(6) Auvin-Guette, C.; Baraguey, C.; Blond, A.; Xavier, H. S.; Pousset, J.-L.; Bodo, B. *Tetrahedron* **1999**, *55*, 11495−11510.
(7) Sabandar, C. W.; Ahmat, N.; Jaafar, F. M.; Sahidin, I. *Phytochemistry* **2013**, *85*, 7−29.
(8) Horswill, A. R.; Benkovic, S. J. *Cell Cycle* **2005**, *4*, 552−555.
(9) Wang, C. K.; Kaas, Q.; Chiche, L.; Craik, D. J. *Nucleic Acids Res.* **2008**, 206−210.
(10) Altei, W. F.; Picchi, D. G.; Abissi, B. M.; Giesel, G. M.; Flausino, O., Jr.; Ravaux-Reboud, M.; Verli, H.; Crusca, E., Jr.; Silveira, E. R.; Cilli, E. M.; Bolzani, V. S. *Phytochemistry* **2014**, *107*, 91−96.
(11) Barbosa, S. C.; Cilli, E. M.; Dias, L. G.; Stabeli, R. G.; Ciancaglini, P. *Amino Acids* **2011**, *40*, 135−144.
(12) Garcia, C. R. S.; Azevedo, M. F.; Wunderlich, G.; Budu, A.; Young, J. A.; Bannister, L. *Int. Rev. Cell. Mol. Biol.* **2008**, *266*, 85−156.
(13) WHO. World Health Organization, 2013. Fact Sheet 94 - Malaria, WHO Media Centre, accessed May 20, 2013, http://www.who.int/mediacentre/factsheets/fs094/en/#.
(14) Brenner, M.; Niederwieser, A.; Pataki, G. In *Dünnschicht-Chromatographie*; Stahl, E., Ed.; Springer-Verlag: New York, 1967; pp 720−721.
(15) Pliss, G.; Zabezhinsky, M. *J. Natl. Cancer Inst.* **1970**, *45*, 283−295.
(16) WenYan, X.; Jun, T.; ChangJiu, J.; WenJun, H.; NingHua, T. *Chin. Sci. Bull.* **2008**, *53*, 1671−1674.
(17) Merrifield, R. B. *J. Am. Chem. Soc.* **1963**, *85*, 2149−2154.
(18) Barron, L. D. *Chirality* **2012**, *24*, 879−893.
(19) Batista, A. N. L.; Batista, J. M., Jr.; Bolzani, V. S.; Furlan, M.; Blanch, E. W. *Phys. Chem. Chem. Phys.* **2013**, *15*, 20147−20152.
(20) Cheeseman, J. R.; Frisch, M. J. *J. Chem. Theory Comput.* **2011**, *7*, 3323−3334.
(21) Craik, D. J. *Science* **2006**, *311*, 1563−1564.
(22) Baraguey, C.; Blond, A.; Cavelier, F.; Pousset, J.-L.; Bodo, B.; Auvin-Guette, C. *J. Chem. Soc., Perkin Trans. 1* **2001**, 2098−2103.
(23) Auvin-Guette, C.; Baraguey, C.; Blond, A.; Lezenven, F.; Pousset, J.-L.; Bodo, B. *Tetrahedron Lett.* **1997**, *38*, 2845−2848.
(24) Auvin-Guette, C.; Baraguey, C.; Blond, A.; Pousset, J.-L.; Bodo, B. *J. Nat. Prod.* **1997**, *60*, 1155−1157.

DOI: 10.1021/np5007668
J. Nat. Prod. 2015, 78, 374−380

(25) Baraguey, C.; Auvin-Guette, C.; Blond, A.; Cavelier, F.; Lezenven, F.; Pousset, J. L.; Bodo, B. *J. Chem. Soc., Perkin Trans. 1* **1998**, 3033−3039.
(26) Baraguey, C.; Blond, A.; Correia, I.; Pousset, J.-L.; Bodo, B.; Auvin-Guette, C. *Tetrahedron Lett.* **2000**, *41*, 325−329.
(27) Frisch, M. J.; Trucks, G. W.; Schlegel, H. B.; Scuseria, G. E.; Robb, M. A.; Cheeseman, J. R.; Scalmani, G.; Barone, V.; Mennucci, B.; Petersson, G. A.; Nakatsuji, H.; Caricato, M.; Li, X.; Hratchian, H. P.; Izmaylov, A. F.; Bloino, J.; Zheng, G.; Sonnenberg, J. L.; Hada, M.; Ehara, M.; Toyota, K.; Fukuda, R.; Hasegawa, J.; Ishida, M.; Nakajima, T.; Honda, Y.; Kitao, O.; Nakai, H.; Vreven, T.; Montgomery, J. A., Jr.; Peralta, J. E.; Ogliaro, F.; Bearpark, M.; Heyd, J. J.; Brothers, E.; Kudin, K. N.; Staroverov, V. N.; Kobayashi, R.; Normand, J.; Raghavachari, K.; Rendell, A.; Burant, J. C.; Iyengar, S. S.; Tomasi, J.; Cossi, M.; Rega, N.; Millam, J. M.; Klene, M.; Knox, J. E.; Cross, J. B.; Bakken, V.; Adamo, C.; Jaramillo, J.; Gomperts, R.; Stratmann, R. E.; Yazyev, O.; Austin, A. J.; Cammi, R.; Pomelli, C.; Ochterski, J. W.; Martin, R. L.; Morokuma, K.; Zakrzewski, V. G.; Voth, G. A.; Salvador, P.; Dannenberg, J. J.; Dapprich, S.; Daniels, A. D.; Farkas, Ö.; Foresman, J. B.; Ortiz, J. V.; Cioslowski, J.; Fox, D. J. *Gaussian 09*, Revision A.02; Gaussian, Inc.: Wallingford, CT, USA, 2009.
(28) Mosmann, T. *J. Immunol. Methods* **1983**, *65*, 55−63.

DOI: 10.1021/np5007668
J. Nat. Prod. 2015, 78, 374−380